Applied Computer Science 2026, vol. 22, no. 2, pp. 138–147
https://doi.org/10.35784/acs_8394

Submitted: 2025-09-17 | Revised: 2026-03-15 | Accepted: 2026-03-23

Keywords: additive manufacturing, robotic 3D printing, optimization, multi-criteria analysis

Łukasz SOBASZEK [1*], *Ivan GAJDOŠ* [2], *Pavol ŠTEFČÁK* [2]
[1] Lublin University of Technology, Poland, l.sobaszek@pollub.pl
[2] Technical University of Kosice, Slovakia, ivan.gajdos@tuke.sk, pavol.stefcak@tuke.sk
[*] Corresponding author: l.sobaszek@pollub.pl

Multi-criteria analysis of parameter impact in large-scale robotic 3D printing

Abstract

Additive manufacturing is widely used for prototyping and producing functional parts. With the growing capabilities of industrial robots, robotic additive manufacturing is becoming an attractive alternative to conventional 3D printing. Robots enable the fabrication of large-scale, structurally complex, and non-planar components that exceed the limitations of traditional printing. However, the flexibility of robotic systems comes with increased complexity in process control – particularly in the selection of appropriate printing parameters, which is critical for ensuring the quality and stability of the printed parts. This paper addresses the need for a systematic approach to parameter selection in robotic 3D printing to ensure optimal process performance and part quality. First, control software to manage and execute the printing process was developed. Secondly, the impact of changes in the industrial robot TCP's velocity and orientation on the quality of manufactured parts was investigated. Furthermore, to optimize the selection of process parameters, the TOPSIS multi-criteria decision-making method was employed. The presented approach provides a methodology for parameter selection and optimization in robotic 3D printing.

1. INTRODUCTION

Additive manufacturing (AM), commonly referred to as 3D printing, has revolutionized the way complex parts are designed and produced across various industries. Traditional 3D printing techniques, typically based on Cartesian coordinate systems and gantry-driven machines, offer precise control and are widely used for small- to medium-sized components (Tkáč et al., 2020). However, these systems often face inherent limitations in terms of build volume, geometric complexity, and process flexibility (Paśnikowska-Łukaszuk et al., 2022).

Due to the limitations of devices operating in the Cartesian coordinate system commonly used in 3D printing (3DP), researchers have begun to explore integrating industrial robots equipped with extruders into AM processes (Yu et al., 2016; Nycz et al., 2018). The key advantage of using robotic systems lies in their increased degrees of freedom and extended working range, which enable the production of larger components (Eyercioğlu & Aladağ, 2021), the fabrication of more complex geometries (Alkhatib, 2023), and, in many cases, the elimination of the need for support structures (Wüthrich et al., 2021). Additionally, industrial robots are equipped with advanced control systems (Vagas & Romancík, 2022), making them well-suited for adaptation to AM processes (Werner et al., 2021).

However, implementing robots in 3DP requires thoughtful adaptation to meet the specific demands of AM technologies. This includes careful selection and integration of devices and actuators, mechanical connection of components to the robot, and incorporation of suitable control systems and software tools for motion execution (Senthil et al., 2023). A key challenge is also the selection of robotic parameters in the robotic 3D printing (robotic 3DP), which is becoming the subject of numerous publications (Csekei et al., 2025).

The field of robotic 3DP is widely studied, with numerous publications proposing different solutions and AM techniques (Bhooshan et al., 2018; Kulikov et al., 2021). Among these, fused deposition modeling (FDM) and fused filament fabrication (FFF) are the most commonly applied methods in robotic systems (Insero et al., 2022). These techniques rely on the deposition of successive layers of molten thermoplastic – typically in filament form such as ABS, PLA, or PET-G – until the desired object is built (Tamir et al., n.d.). Their popularity is due to low production costs, good mechanical strength, post-processing capabilities, and the water resistance of the printed parts (Kristiawan et al., 2021). Given the large-scale nature of many robotic

3DP applications, an increasingly popular variation is screw-extrusion additive manufacturing (SEAM), which uses plastic pellets rather than filament as feedstock material (Li et al., 2024). Beyond FDM/FFF and SEAM, a variety of novel approaches have been proposed in robotic 3DP. For example, Kulikov et al. (2021) present a case study on programming industrial robots for metal additive manufacturing, reflecting the growing interest in robotic metal printing. Other emerging areas include the use of cementitious and composite materials (Puzatova et al., 2022), with concrete 3DP being a particularly active area of research (Bhooshan et al., 2018). Due to the unique properties of such materials, researchers are continually developing and adapting printing systems (Tiryaki et al., 2019; Zhang et al., 2018). One notable example is the mobile robotic 3DP system described in McPherson et al. (2017), which highlights the importance of collaborative robotic solutions in shared printing environments (McPherson & Zhou, 2018). Ongoing development in this area is further demonstrated by innovations such as collision-free polygon mesh printing (Yu et al., 2016) and the implementation of collaborative robots in robotic 3DP workflows.

Regardless of the specific additive manufacturing technology employed, the selection of appropriate process parameters remains a critical factor influencing the quality and performance of printed parts. In the context of robotic 3DP, this aspect becomes even more important, as the process is not yet as mature or standardized as conventional Cartesian-based 3D printing. Existing guidelines and parameter databases for classic 3D printers cannot be directly applied to robotic systems due to differences in kinematics, motion control, and material deposition dynamics (Pulquerio et al., 2024). As a result, extensive experimentation and systematic parameter optimization are required to achieve consistent and reliable outcomes (Csekei et al., 2025). Addressing this challenge is essential for unlocking the full potential of robotic 3DP in industrial applications.

Unlike existing studies focusing primarily on process parameter tuning or simulation-based optimization, the proposed approach integrates experimental validation with multi-criteria decision-making using the TOPSIS method. The main objective of the research presented in this publication was to identify the impact of selected parameters on the robotic 3DP process for large-sized parts. The primary criterion of the study was to examine how the selected parameters affect the quality of the fabricated surfaces, the continuity of the material, and the accuracy of curvature reproduction. For this purpose, a control tool for the robotic 3DP process was developed in MATLAB. The manufacturing process was carried out with various parameter settings, and the TOPSIS method was subsequently applied to conduct a multi-criteria analysis of the process and support parameter selection.

2. METHODS

2.1. Experimental setup

To investigate the impact of parameter values on components manufactured using robotic 3DP, dedicated experiments were conducted on a specialized robotic workstation. The robotic AM workstation (Figure 1) consisted of a FANUC M-20iB robot, a Massive Dimension MDPH2 pellet head extruder, an Industrial Shields M-Duino 57R I/Os PLUS PLC, and a heating bed. Utilized printing technology was SEAM.

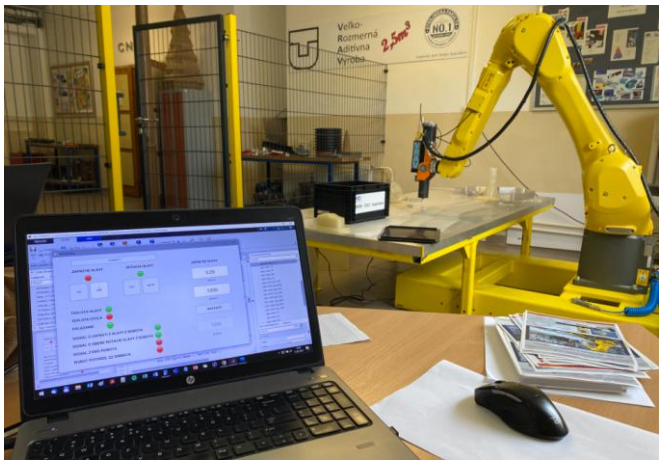

Fig. 1. Robotic 3DP workstation utilized during research

The main points of the research included:

1. Communication solutions between the industrial robot controller and the extruder tool development.
2. Research on the impact of changes of velocity and orientation of the TCP of the industrial robot on the quality of manufactured parts.
3. Evaluation of parts produced with alternative operating parameter values of key process devices.

The proposed research began with the development of a methodology for implementing communication between a robot and its tool. In that field, MATLAB software and dedicated libraries were used to integrate the devices (Figure 2). In this area, the typical communication protocol, Modbus, has been used. Developed software that worked properly and allowed for control of process parameters during the implementation of subsequent program parts.

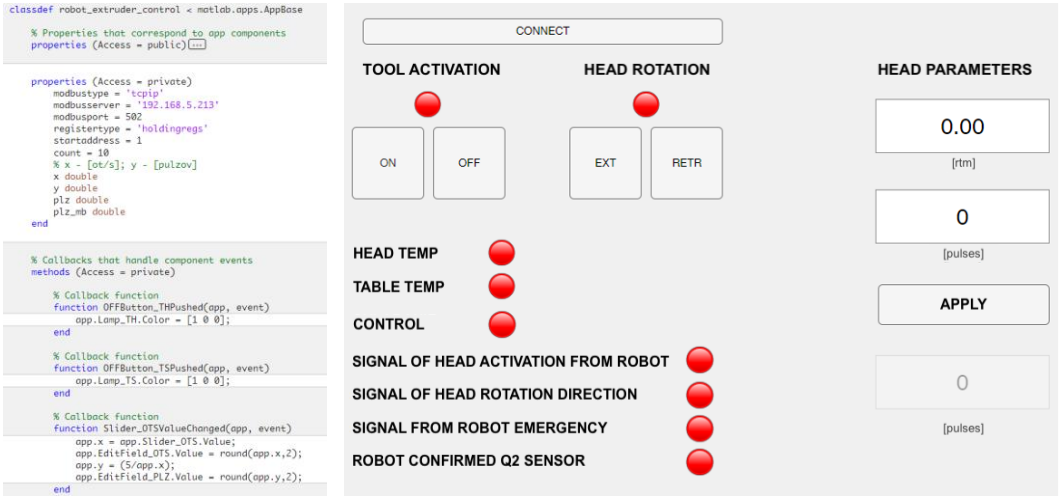

Fig. 2. Developed software code fragment and GUI

In the field of research on the impact of changes in velocity and orientation of the TCP of the robot, the 3D printing process for thin-walled parts with curved shapes was analyzed. First of all, an appropriate STL model was prepared using Rhinoceros 3D software and the Grasshopper plugin (Figure 3).

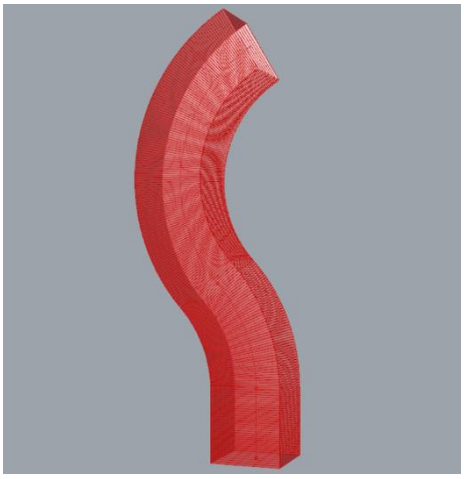

Fig. 3. Thin-walled part developed in Rhinoceros 3D to generate a point cloud for a STL model

2.2. Simulation and real-world experiments

The research involved simulating a robot carrying out additive manufacturing processes in a virtual robot development environment was conducted. The RoboDK OLP (offline programming) software was utilized to validate properties of developed control codes (Figure 4). Based on the built-in 3D Printing Project tool utilized, it was possible to implement the generated G-Code and observe the robot's operation. The process was aimed at checking the movements of the robot tool in the individual layers of the manufactured part.

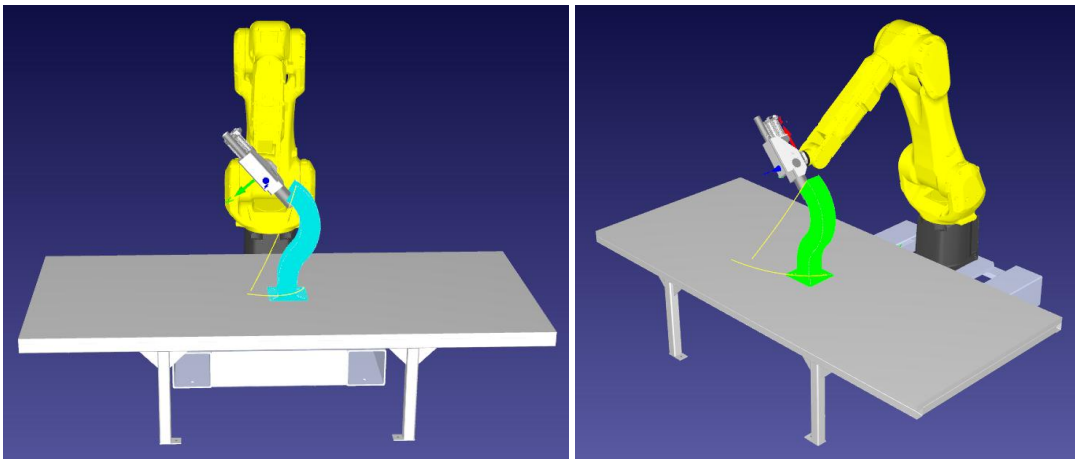

Fig. 4. RoboDK robotic simulation environment – robot control code generation and process simulation

The process under consideration was conducted on the real workstation with the parameters presented in Table 1. Models 1–3 were printed with constant robot velocity and TCP orientation (the extruder was oriented as in classic 3D printers). Models 4–6 were printed with varying values of the aforementioned parameters.

Tab. 1. Parameters of the conducted robotic 3DP processes

Model no.	**Nozzle diameter** [mm]	**Orientation of the TCP** [–]	**Layer height** [mm]	**Robot velocity** [mm/s]	**Melt temperature** [°C]	**Extrusion rate (delay of motor impulses)** [ms]	**Material** [–]
Model 1	1.5	constant	0.56	25	220	1100	PETG
Model 2	1.5	constant	0.75	25	220	850	PETG
Model 3	1.5	constant	0.98	25	220	500	PETG
Model 4	1.5	variable	0.56	40	220	1100	PETG
Model 5	1.5	variable	0.75	32	220	980	PETG
Model 6	1.5	variable	0.98	20	220	640	PETG

The last part of the research presented an evaluation of parts produced under alternative operating parameter values for key process devices. For this purpose, the TOPSIS method (Technique for Order Preference by Similarity to an Ideal Solution) was applied. The technique mentioned is among the most commonly used multi-criteria analysis methods. Its use enabled a detailed analysis of the obtained results and the identification of an appropriate set of process parameters. By measuring the relative closeness to an ideal solution, TOPSIS helps identify the most balanced option among the available alternatives (Zhang et al., 2024).

3. RESULTS

3.1. Experimental results of robotic 3DP

Based on the manufactured models, it should be noted that a constant robot tool angle is not a suitable solution for the additive manufacturing of large-sized parts (Figure 5). In each case, the models were executed correctly only up to a few layers of curvature; after that, visible delamination of the layers was observed (Figure 6A). The obtained surface quality was average, and material continuity was very good (there was no air inclusions). However, the representation of the curves was poor (Figure 6B). The average deviation in size measured at a distance of 1 cm from the base ranged from 0.1 to 0.35 mm.

Model number 2 (Figure 5) was manufactured to the highest quality standards. However, due to the parameters chosen, it was not produced correctly until the end. It can be concluded that in the manufacturing of large-sized thin-walled parts, it is crucial to change the robot tool orientation and adjust the velocity. In analyzing its structure, it should be noted that the key parameter of the process is also the choice of an appropriate extrusion rate.

Fig. 5. Models obtained – constant value of the robot tool angles

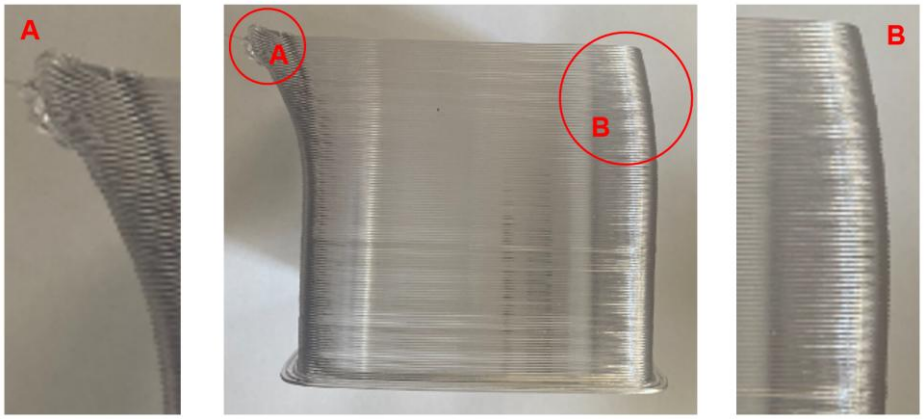

Fig. 6. Detailed structure of the model 1 – delamination (detail A) and visibility of the layers (detail B)

Considering the structure of the obtained models, it should be noted that the variable robot tool angles allow for achieving better models of manufactured large-sized parts. In each case, the models were correctly manufactured, and no delamination of the layers was observed (Figure 7). The obtained surface quality was good, and material continuity was good or average. In several locations, air inclusions were observed (Figure 8B). What is very important, the representation of the curves was good (Figure 8A). However, the average deviation in size measured at a distance of 1 cm from the base ranged from 0.60 to 0.85 mm.

Fig. 7. Models obtained – variable values of the robot tool angles

3.2. Multi-criteria optimization using the TOPSIS method

The last part of the research presented an evaluation of parts produced under alternative operating parameter values for key process devices. The results obtained were summarized in Table 2, and the TOPSIS method was applied. The technique mentioned is among the most commonly used multi-criteria analysis methods. For

the purpose of accessible multi-criteria analysis and straightforward interpretation of the obtained results, the aforementioned technique was implemented in the RStudio environment using appropriate libraries.

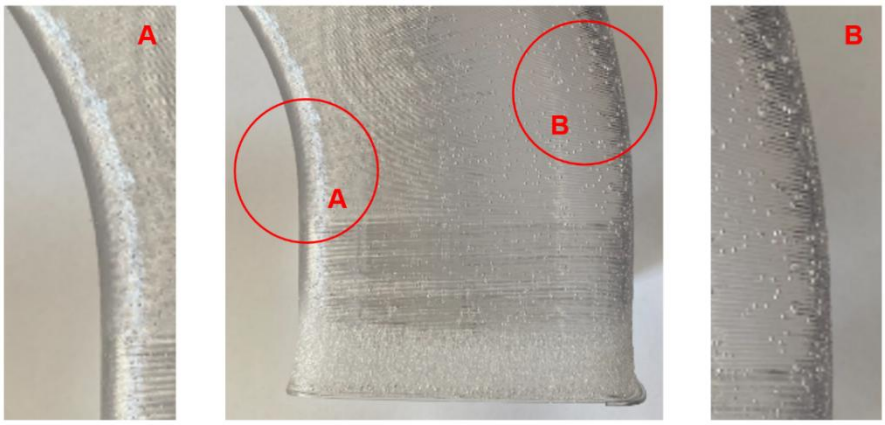

Fig. 8. Detailed structure of the model 5 – proper representation of the curves (detail A) and air inclusion (detail B)

Tab. 2. Summary of research results

Model no.	**Layer height** [mm]	**Printing speed** [mm/s]	**Extrusion rate (delay of motor impulses)** [ms]	**Dimension deviation**[mm]	**Surface quality** [–]	**Material continuity** [–]	**Curvatures** [–]
Model 1	0.56	25	1100	0.20	average	very good	poor
Model 2	0.75	25	850	0.10	average	very good	poor
Model 3	0.98	25	500	0.35	average	very good	poor
Model 4	0.56	40	1100	0.85	good	average	good
Model 5	0.75	32	980	0.60	good	good	good
Model 6	0.98	20	640	0.75	average	average	average

To express all parameters using a numerical scale and select the best parameter set as As a consequence, the assumption was stated. For the parameters *Surface quality*, *Material continuity*, and *Curvature* values were as follows: poor – 1, average – 2, good – 3, very good – 4. Based on the obtained data, the vector performance value was calculated, and, based on this value, the normalization matrix was determined. Moreover, to outline the key role of the parameters representing the quality of the manufactured elements, the appropriate weights were assumed (Table 3).

Surface quality and material continuity were selected as key indicators of structural integrity, while dimension deviation was considered a minimization criterion reflecting geometric accuracy. The weights were assigned based on the relative importance of the parameters in large-scale thin-walled structures, with higher priority given to curvature representation and dimensional accuracy.

Tab. 3. Considered parameters assumed values

Model no.	**Layer height** [mm]	**Printing speed** [mm/s]	**Extrusion rate (delay of motor impulses)** [ms]	**Dimension deviation** [mm]	**Surface quality** [–]	**Material continuity** [–]	**Curvatures** [–]
Model 1	0.56	25	1100	0.20	2	4	1
Model 2	0.75	25	850	0.10	2	4	1
Model 3	0.98	25	500	0.35	2	4	1
Model 4	0.56	40	1100	0.85	3	2	3
Model 5	0.75	32	980	0.60	3	3	3
Model 6	0.98	20	640	0.75	2	2	2
Weight:	**0.0**	**0.15**	**0.1**	**0.15**	**0.2**	**0.15**	**0.25**

As a consequence, the performance score (*Pi*) based on ideal best values, ideal worst values, and the distances from those values (*S*+ and *S*–) was determined. During the calculations, it was also defined which of

the considered parameters should be maximized and which minimized. In the present study, the only minimization criterion was *Dimension Deviation.* This allowed us to rank the solutions and select the best one (Table 4).

Tab. 4. Weighted matrix of normalization

Model no.	*S*+	*S*–	*Pi*	Rank
Model 1	0.043729	0.028297	0.392870	4
Model 2	0.043786	0.029426	0.401928	3
Model 3	0.045072	0.024123	0.348625	5
Model 4	0.028857	0.045086	0.609740	2
Model 5	**0.017923**	**0.045510**	**0.717449**	**1**
Model 6	0.038976	0.020305	0.342523	6

To analyze the results in an accessible way, they were visualized using a heat map and a radar chart. The heat map (Figure 9) presents the normalized values of seven evaluation criteria across the considered models (M1–M6). Warmer colors (red/orange) indicate higher-than-average values, while cooler colors (blue/purple) reflect lower-than-average values. For maximization criteria such as *Surface Quality* and *Material Continuity*, warmer tones are desirable, whereas for minimization criteria like *Dimension Deviation*, cooler tones are preferred. Model no. 4 demonstrates strong performance in several maximization criteria but performs poorly in *Dimension Deviation*, highlighting the need for a balanced trade-off in multi-criteria decision-making.

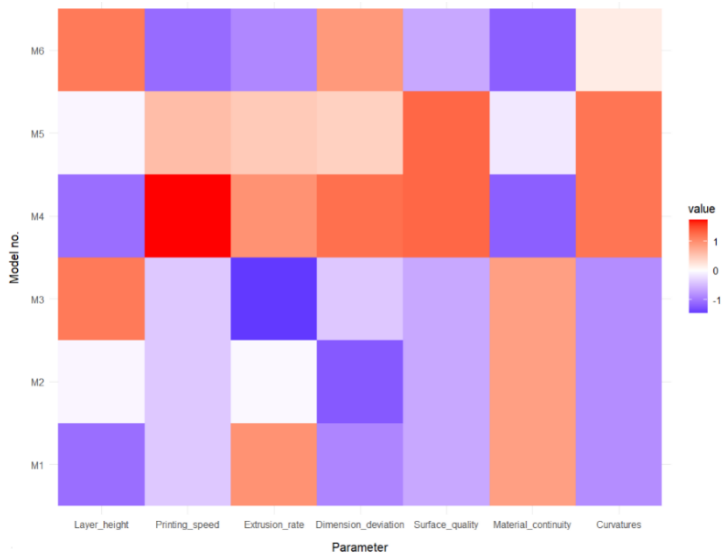

Fig. 9. Heat map of normalized values

The radar chart illustrates the performance profiles of the models across evaluation criteria (Figure 10). Model no. 5 exhibits an extended area across most axes, demonstrating strong and consistent performance. The other models indicate that smaller or skewed shapes reveal trade-offs or deficiencies in specific attributes. The chart confirms the calculations and demonstrates that, in the multi-criteria analysis, the criteria for the robotic 3DP process are most favorable for manufacturing model no. 5.

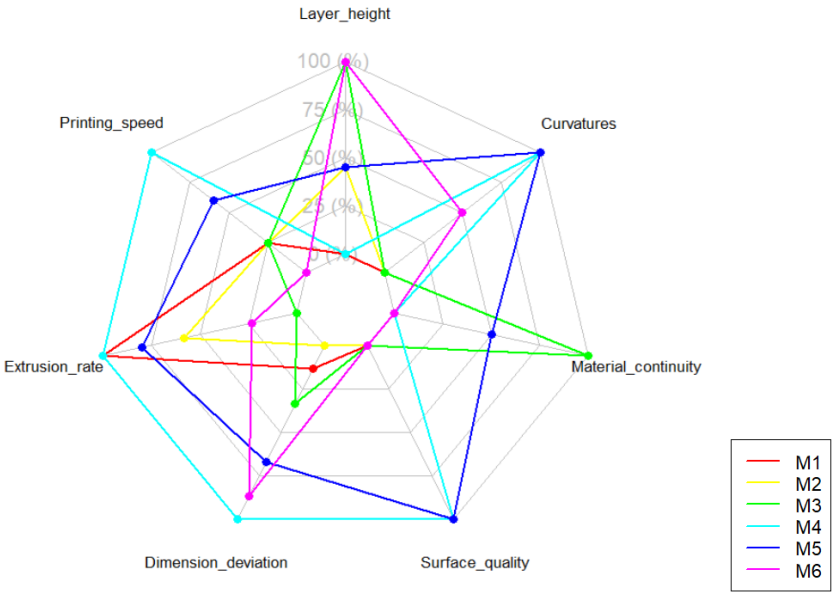

Fig. 10. Radar chart of the considered models

The presented study is subject to several limitations. First, the analysis was conducted on a limited number of parameter sets (Models 1–6), which may restrict the generalizability of the results. Second, the experiments were performed using PETG, and the observed behavior, particularly regarding layer adhesion and air inclusions (Figures 6 and 8), may differ from other materials. Moreover, the results indicate a strong dependence of manufacturing quality on the robot tool orientation and extrusion rate, both of which require dynamic adjustment during the process.

Despite these limitations, the proposed approach can be extended to other robotic additive manufacturing scenarios. The combination of experimental evaluation and TOPSIS-based multi-criteria optimization provides a flexible framework for selecting process parameters under different technological conditions. Therefore, the methodology can be adapted to various materials, geometries, and robotic systems.

4. DISCUSSION

Based on the results obtained, it should be stated that the best parameters were assumed in manufacturing model 5. The experiments showed that maintaining constant robot tool angles is unsuitable for large-scale additive manufacturing. Models built with this approach failed after the first curved layers due to delamination. Although material continuity was good and dimensional deviation remained low (0.10–0.35 mm), the surface quality was only average, and curved features were poorly reproduced. This highlights the need for dynamic adjustment of tool orientation, velocity, and extrusion rate in large-scale thin-walled builds.

In contrast, variable tool angles yielded better overall results. No delamination was observed, surface quality was generally good, and curves were reproduced accurately. Minor air inclusions were present, and dimensional deviation increased to 0.60–0.85 mm, indicating a trade-off between structural cohesion and geometric precision.

The TOPSIS analysis, supported by heat map and radar chart visualizations, confirmed the trade-offs between criteria. Model 5 achieved the most balanced performance, combining good surface properties, structural integrity, and dimensional accuracy. To sum up, the best parameters for the manufacturing process of robotic thin-walled parts with curved shapes are: material: PETG, nozzle diameter: 1.5 mm, melt temperature: 220 °C, layer height: 0.75 mm, printing speed: 32 mm/s, extrusion rate: 980 ms, orientation of robot TCP: variable.

5. CONCLUSIONS

Due to the limitations of devices commonly used in conventional 3D printing, increasing attention has been paid to integrating industrial robots equipped with extruders into AM processes. The main advantage of robotic

systems lies in their greater degrees of freedom and extended working range, which enable the production of larger components, the fabrication of more complex geometries, and, in many cases, the elimination of the need for support structures.

This study highlights the necessity of a systematic approach to parameter selection for robotic 3DP to ensure optimal process performance and high-quality parts. As a result of the conducted research, it was found that maintaining constant robot tool angles is not suitable for large-scale additive manufacturing, as it leads to layer delamination despite acceptable material continuity and dimensional accuracy. In contrast, variable tool orientation improved surface quality, cohesion, and curve reproduction, although it increased dimensional deviation, highlighting a trade-off between geometry and structural integrity. The results also indicated that extrusion rate and velocity are key parameters influencing the process outcome. By applying the TOPSIS method, it was possible to balance competing criteria and identify the most appropriate model as the favorable solution. Overall, the findings emphasize the need for dynamic parameter adjustment and the use of multi-criteria decision-making tools to optimize robotic 3DP of large thin-walled components. However, optimization is required to balance surface finish and dimensional precision, with multi-criteria methods such as TOPSIS providing effective support in selecting optimal parameter sets.

The presented research will be further developed, with particular attention given to a detailed analysis of individual parameters, such as tool inclination angle. Future work should therefore focus on expanding the study and incorporating AI-based methods to support the selection of optimal process parameters.

Conflicts of Interest

The authors declare no conflict of interest.

REFERENCES

Alkhatib, T. (2023). *Robotic 3D printing of sustainable structures* [Thesis]. Linnaeus University.

Bhooshan, S., Ladinig, J., Van Mele, T., & Block, P. (2019). Function representation for robotic 3D printed concrete. In J. Willmann, P. Block, M. Hutter, K. Byrne, & T. Schork (Eds.), *Robotic fabrication in architecture, art and design 2018*. Springer. https://doi.org/10.1007/978-3-319-92294-2_8

Csekei, M., Šido, J., Nižňan, P., Ružarovský, R., Zelník, R., & Michal, D. (2025). Optimization of parameters in robotic additive manufacturing of thinwalled tubes: Experimental analysis and path planning. *MM Science Journal*, 8204–8210. https://doi.org/10.17973/MMSJ.2025_03_2025012

Eyercioğlu, Ö., & Aladağ, M. (2021). Non-planar toolpath for large scale additive manufacturing. *International Journal of 3D Printing Technologies and Digital Industry, 5*(3), 477–487. https://doi.org/10.46519/ij3dptdi.956313

Insero, F., Furlan, V., & Giberti, H. (2022). A novel infill strategy to approach non-planar 3D-printing in 6-axis robotized FDM. *IEEE/ASME International Conference on Mechatronic and Embedded Systems and Applications (MESA)* (pp. 1-6). IEEE. https://doi.org/10.1109/mesa55290.2022.10004465

Kristiawan, R. B., Imaduddin, F., Ariawan, D., Ubaidillah, N., & Arifin, Z. (2021). A review on the fused deposition modeling (FDM) 3D printing: Filament processing, materials, and printing parameters. *Open Engineering, 11*(1), 639–649. https://doi.org/10.1515/eng-2021-0063

Kulikov, A. A., Sidorova, A. V., & Balanovskii, A. E. (2021). Programming industrial robots for wire arc additive manufacturing. In *Lecture Notes in Mechanical Engineering* (pp. 566–576). Springer. https://doi.org/10.1007/978-3-030-54817-9_66

Li, X., Liu, W., Hu, Z., He, C., Ding, J., Chen, W., Wang, S., & Dong, W. (2024). Supportless 3D-printing of non-planar thin-walled structures with the multi-axis screw-extrusion additive manufacturing system. *Materials & Design, 240*, 112860. https://doi.org/10.1016/j.matdes.2024.112860

McPherson, J., & Zhou, W. (2018). A chunk-based slicer for cooperative 3D printing. *Rapid Prototyping Journal, 24*(9), 1436–1446. https://doi.org/10.1108/rpj-07-2017-0150

McPherson, J., Bliss, A., Smith, F., Hariss, E., & Zhou, W. (2017). A slicer and simulator for cooperative 3D printing. In *Solid Freeform Fabrication 2017: Proceedings of the 28th Annual International Solid Freeform Fabrication Symposium – An Additive Manufacturing Conference*. https://repositories.lib.utexas.edu/handle/2152/89887

Nycz, A., Noakes, M. W., Masuo, C. J., & Love, L. J. (2018). Control system framework for using g-code-based 3D printing paths on a multi-degree of freedom robotic arm. In *Solid Freeform Fabrication 2018: Proceedings of the 29th Annual International Solid Freeform Fabrication Symposium – An Additive Manufacturing Conference, SFF 2018*. https://doi.org/10.26153/tsw/17155

Paśnikowska-Łukaszuk, M., Korulczyk, K., Kapłon, K., Urzędowski, A., & Wlazło-Ćwiklińska, M. (2022). Time distribution analysis of 3D prints with the use of a filament and masked stereolithography resin 3D printer. *Advances in Science and Technology Research Journal, 16*(5), 242–249. https://doi.org/10.12913/22998624/154926

Pulquerio, E. C., Barbosa, G. F., & Shiki, S. B. (2024). Robotic additive manufacturing system: Development of suitable range of process parameters for 3D printing of a large-sized object in PLA polymer. *Progress in Additive Manufacturing, 10*(1), 887–898. https://doi.org/10.1007/s40964-024-00123-4

Puzatova, A., Shakor, P., Laghi, V., & Dmitrieva, M. (2022). Large-scale 3D printing for construction application by means of robotic arm and gantry 3D printer: A review. *Buildings, 12*(11), 2023. https://doi.org/10.3390/buildings12112023

Senthil, T. S., Vel, N. R. O., Puviyarasan, M., Babu, S. R., Surakasi, R., & Sampath, B. (2023). Industrial robot-integrated fused deposition modelling for the 3D printing process. In *Advances in Chemical and Materials Engineering Book Series* (pp. 188–210). https://doi.org/10.4018/978-1-6684-6009-2.ch011

Tamir, T. S., Xiong, G., Shen, Z., Leng, J., Fang, Q., Yang, Y., Jiang, J., Lodhi, E., & Wang, F. Y. (2023). 3D printing in materials manufacturing industry: A realm of Industry 4.0. *Heliyon, 9*(10), Article e19689. https://doi.org/10.1016/j.heliyon.2023.e19689

Tiryaki, M. E., Zhang, X., & Pham, Q. (2019). Printing-while-moving: A new paradigm for large-scale robotic 3D printing. In *International Conference on Intelligent Robots and Systems (IROS)*. https://doi.org/10.1109/iros40897.2019.8967524

Tkáč, J., Samborski, S., Monková, K., & Dębski, H. (2020). Analysis of mechanical properties of a lattice structure produced with the additive technology. *Composite Structures, 242*, Article 112138. https://doi.org/10.1016/j.compstruct.2020.112138

Vagas, M., & Romancík, J. (2022). Testing of Ethernet-based communication between control PLC and collaborative mechatronic system. In D. Maga & J. Hajek (Eds.), *Proceedings of the 20th International Conference on Mechatronics – Mechatronika (ME)* (pp. 1-4). IEEE. https://doi.org/10.1109/ME54704.2022.9983428

Werner, J., Aburaia, M., Raschendorfer, A., & Lackner, M. (2021). MeshSlicer: A 3D-printing software for printing 3D-models with a 6-axis industrial robot. *Procedia CIRP, 99*, 110–115. https://doi.org/10.1016/j.procir.2021.03.018

Wüthrich, M., Gubser, M., Elspass, W. J., & Jaeger, C. (2021). A novel slicing strategy to print overhangs without support material. *Applied Sciences, 11*(18), 8760. https://doi.org/10.3390/app11188760

Yu, L., Huang, Y., Zhongyuan, L., Xiao, S., Liu, L., Song, G., & Wang, Y. (2016). Highly informed robotic 3D printed polygon mesh: A novel strategy of 3D spatial printing. *ACADIA Quarterly*, 298–307. https://doi.org/10.52842/conf.acadia.2016.298

Zhang, L., Wang, X., & Gao, M. (2024). Optimizing additive manufacturing parameters for graphene-reinforced polymer composites: a Fuzzy AHP–TOPSIS approach. *Journal of Manufacturing Processes, 80*, 123–132. https://doi.org/10.1016/j.jmapro.2024.03.006

Zhang, X., Li, M., Lim, J. H., Weng, Y., Tay, Y. W. D., Pham, H., & Pham, Q. (2018). Large-scale 3D printing by a team of mobile robots. *Automation in Construction, 95*, 98–106. https://doi.org/10.1016/j.autcon.2018.08.004